

Xian Wu¹
 Mei Li²
 Jian Li²
 Yanwei Liu¹
 Hao Zhang³
 Hongxin Li¹
 Zongzhi Lu^{1*}

Machine Learning-Based Remote Sensing Monitoring and Prediction Modeling Of *Bolboschoenus planiculmis*



Abstract: - A multivariate regression approach is utilized to map the geographical dispersion of Above-ground biomass (AGB) of *Bolboschoenus planiculmis* (*B. planiculmis*) using simultaneous moderate spatial resolution satellite images and field data. *Bolboschoenus planiculmis* stands as an essential target species of plants for rehabilitation of damaged wetlands in the Momoge National Nature Reserve (MNNR), China's northeast. Initially the information is collected from Operational Land Imager (OLI) dataset, and then the collected data are fed to pre-processing segment. In pre-processing, Multi-window Savitzky-Golay Filtering (MWSGF) is used to preprocess the data to enhance image clarity. Then the preprocessed output is fed to Historical Information Passing Networks (HIPNs) is successfully used to predict the AGB of *B. planiculmis*. In general, Historical Information Passing Networks (HIPNs) the classifier does not articulate ways for optimizing parameters to guarantee accuracy AGB of *B. planiculmis* prediction. Hence, proposed FLO enhances Historical Information Passing Networks (HIPNs), accurately predict the AGB of *B. planiculmis*. The weight parameter of the HIPN optimized with FLO for accurate prediction. The proposed RSPB-HIPN-FLO proposed is implemented on the Python working platform. The performance of proposed method examined utilizing performance metrics likes accuracy, precision; Root Mean Squared Error, Mean Absolute Error, and Correlation Coefficient were looked at. A suggested RSPB-HIPN-FLO approach contains 23.52%, 21.72% and 24.92% higher accuracy; 23.52%, 22.72% and 21.92% higher Precision; and 24.58%, 21.71% and 22.90% lower and Root Mean Squared Error likened with current methods, like Monitoring invasive plant species using hyper spectral remote sensing data (PSHRS-ANN), Combining machine learning and remote sensing-integrated crop modeling for rice and soybean crop simulation (RSICS-DNN) and GOA-optimized deep learning for soybean yield estimation using multi-source remote sensing data (SYMRS-GOA) respectively..

Keywords: *Bolboschoenus Planiculmis*, Food Plant, Growth Strategy, Historical Information Passing Networks, Landsat, Remote Sensing, Operational Land Imager.

I. INTRODUCTION

a) Background

Coastal wetlands stand out as the most prosperous of the various marine environments. The way plant efficiency is spread throughout these wetlands holds significance for nutrient cycling, as well as for providing essential habitat and food for wildlife [1]. Particularly crucial are the primary producers equipped with specialized nutrient storage organs such as tubers and rhizomes, as they play a vital role in attracting herbivores, including endangered migratory waterfowl [2]. Traditionally, the spatial distribution of *B. planiculmis* inspecting every plant to evaluate coastal plants within predetermined areas at specified intervals. Nevertheless, such point measurements may not fully capture the varying patterns and geographical complexity of coastal vegetation [3]. Additionally, carrying out spatial interpolation point surveys proves labor-intensive, also accumulating sufficient validation points on a mudflat poses challenges [4]. A method involving the scanning of individual leaf images for estimating shoot biomass has been proposed recently, yet it shares analogous constraints with point measurements [5]. Challenges arise with these field assessments when endeavoring to cover expansive areas, requiring surveyors to transport cumbersome instruments to each point. Specifically, conducting surveys over extensive mudflat terrain with heavy equipment proves exceedingly labor-intensive [6]. An additional method for determining the geographical distribution of different plant attributes is the use of remotely sensed photography, which has demonstrated success in a variety of habitat types [7, 8]. However, monitoring vegetation in coastal areas using remote sensing methods poses additional challenges compared to

¹Institute of Plant Protection, Jilin Academy of Agricultural Sciences, Changchun, China, 130000

²Institute of Plant Protection, ShanDong Academy of Agricultural Sciences, Jinan, China, 250100

³ College of Plant Protection, Jilin Agricultural University, Changchun, China, 130118

*Corresponding author e-mail: zongzhiluphd@gmail.com

estrial ecosystems like forests and grasslands [9]. Estuarine wetlands typically experience high turbidity in their water, caused by suspended solid particles, which disrupts the vegetation's spectral reflectance. Some plants in the intertidal zone that are completely buried at high tide, prove challenging to detect due to water reflectance and surface scattering [10].

b) Literature Review

Various research works have previously existed in the literature which is based on deep learning; the remote sensing monitoring and prediction based on deep learning and aspects. Some of them are reviewed here,

Levente Papp et al. [11] have suggested that a PSHRS-ANN. The biodiversity and species richness of Hungary's vegetation face escalating threats from aggressive plant species introduced from other landmasses and distant ecosystems. In Europe, these aggressive species had expanded rapidly on both usual and semi-natural ecosystems. Mutual milkweed is one among them (*Asclepias syriaca*) stands out as one of the most ecologically menacing species. Hence, this study aims to chart and watch a proliferation of mutual milkweed, the predominant Herb varieties that are aggressive in Europe. Additionally, it explores the feasibility of detecting and validating this invasive species using hyperspectral remote sensing information. High-resolution hyperspectral aerial pictures, captured with an autonomous aerial vehicle (UAV) system with 138 haunted groups, were analyzed on common milkweed-infested zones, alongside field reference data. Subsequently, support vector machine (SVM) and artificial neural network (ANN) categorization procedures on the carefully gathered field orientation information. This technique yields poor precision and great accuracy.

Jonghan Ko et al. [12] have developed that a machine learning approach to estimate Leaf Area Index (LAI) using data from proximate sensing in the rice and soybean crops. Additionally, assessed the presentation of a Remote Sensing-Integrated Crop Model (RSCM) was combined by machine learning procedures. The analyzed datasets from rice and soybean crops to determine the maximum suitable machine learning procedures for demonstrating the correlation among LAI and flora directories resultant from awning reflectance capacities. This method provides high Correlation Coefficient and low precision.

Jian Lu et al. [13] have presented that a deep learning framework specializes in accurately estimating county-level soybean yields in the United States, leveraging an extensive array of multi-variable remote sensing data. Improved by the GOA and a novel attention mechanism (GCBA), the CNN-BiGRU example represents a state-of-the-art architecture adept at managing complex time series with various datasets from remote sensing. This method provides high accuracy and high Root Mean Squared Error.

Javaid et al. [14] have suggested that a remote sensing in agriculture to increase sustainability, resource efficiency, and production. The combination of remote sensing techniques with sophisticated data analysis methodologies, such as satellite images, aerial photography, and sensor-based data collection. This method provides high accuracy and high Mean Absolute Error.

Hau-Hsuan Hwang et al. [15] have developed that a Severe drought and soil salinization from rising temperatures have been made worse by an increase in extreme weather occurrences brought on by climate change and global warming. In the face of numerous abiotic stressors, these environmental obstacles impede commercially significant crop output, plant growth, and development. One can isolate entophytic bacteria from surface-sterilized plant tissues if they are present in the host plant but do not appear to be harmful. An alternative strategy to conventional breeding and genetic modification methods for choosing or developing fresh harvest varieties resilient to various ecological stresses is to use these plant entophytic microorganisms to improve growth and tolerance to stress of plants in surroundings. This method provides high accuracy and low precision.

Hyunyoung Yang et al. [16] have suggested that a impacts effects embankments-induced tidal limitation on the plastic reactions to growth of *Bolboschoenus planiculmis* in Korea. Tidal restrictions caused by embankments can significantly impact estuarial ecosystems by altering tidal regimes, thereby influencing the expansion and maturation of marsh vegetation. Even so, there are extensive tidal freshwater marshes in Korea around the Yellow Sea may experience both negative and positive effects due to embankments, little was understood about how tidal restrictions affect the plastic evolution responses of swamp plants, potentially leading to population declines in the field. This method provides high Correlation Coefficient and low precision.

Hyunyoung Yang et al. [17] have presented that impact of the impact of tides on interspecific relationships and *Bolboschoenus planiculmis* plastic reactions to growth were evaluated. The kind of interspecific interactions among *B. planiculmis* and *Carex scabrifolia* was changed by simulated tide; for *B. planiculmis*, the communication was neutral in the tidal handling, but negative (competitive) in the nontribal treatment.

Interspecific interactions and tide both contributed to a decline in *B. planiculmis* biomass. Reduced sexual reproduction in *B. planiculmis* and thinner stems were noted under tidal circumstances, which is consistent with an avoidance strategy; no other plastic growth responses were noted. In response to tidal stress, *Carex scabifolia* showed a reduction in biomass but no plastic ability. This method provides high precision and high Mean Absolute Error.

c) Research Gap and Motivation

A general assessment of current research indicates that machine learning-based remote sensing monitoring and prediction modeling of *Bolboschoenus planiculmis*. Point measurements, however, may not accurately capture the diversity and complexity of coastal vegetation throughout space. Furthermore, gathering enough validation points on a mudflat is challenging because point surveying is time-consuming for spatial interpolation. Numerous scholars address the issue of various technologies in literature, like ANN, deep neural network (DNN) and Grasshopper Optimization Algorithm (GOA). The ANN models for hyper spectral data analysis necessitate significant computational power and expertise in both neural network architecture design and parameter optimization. Additionally, the effectiveness of ANN models can be affected by issues such as overfitting, which may arise when the model captures noise in the training data rather than meaningful patterns, leading to decreased generalization performance. The potential complexity and interpretability challenges associated with DNN models pose a consideration in utilizing crop modeling for rice and soybeans that integrates machine learning and remote sensing. DNNs are highly intricate models with numerous layers of interconnected neurons, rendering them computationally intensive and necessitating substantial resources for training and deployment. SYMRS-GOA is the potential challenge of data acquisition and preprocessing. Integrating data from multiple remote sensing sources requires meticulous preprocessing to ensure consistency and compatibility across datasets. This process may involve addressing differences in spatial and spectral resolutions, as well as dealing with missing or noisy data. These disadvantages serve as the driving force behind this study.

d) Challenges

In estimating the AGB of tuberous bulrush (*Bolboschoenus planiculmis*) using remotely sensed multispectral imagery in mudflats, several challenges arise. These include accurately delineating the boundaries of the target species amidst diverse wetland vegetation, accounting for variations in biomass density across different mudflat areas, and addressing the influence of environmental factors such as water depth and soil moisture content on biomass estimation accuracy. Additionally, ensuring the reliability and consistency of remote sensing data acquisition and processing methods while accounting for seasonal changes and image artifacts presents further complexities. Overcoming these challenges necessitates the development of robust analytical techniques, integration of ancillary data sources, and validation through ground-truthing efforts to improve the precision and reliability of biomass estimation for effective wetland management strategies.

e) Contribution

The following list summarizes the important contributions of this manuscript:

- Initially data gathered from OLI dataset.
- To reduce noise and enhance image clarity, a Multi-window SG Filtering is applied in the pre-processing section.
- The Historical Information Passing Network then receives the pre-processed data and used to predict AGB of *B. planiculmis*.
- The historical information passing neural network's weight parameter is optimized using the FLO to enhance the HIPN.
- The proposed RSPB -HIPN- FLO method is applied, and presentation metrics like correctness, precision, Examined are the association coefficient, mean total error, and root mean square error.

f) Organization

Section 1 describe the introduction is explain the literature review and background of the research work, the suggested approach is obtainable in Section 2, the findings and discussion are accessible in Section 3, the Deduction is made clear in Section 4, and the text is decided in Section 4.

II. PROPOSED METHODOLOGY

It suggests methodology RSPB-HIPN-FLO. The OLI dataset offers high-resolution imagery for comprehensive land monitoring, aiding in environmental assessment and resource management. The OLI dataset facilitates timely decision-making for agriculture, forestry, and urban planning applications. Multi-

window SG is used at the pre-processing stage to decrease sound and improve image clarity. An output of predict stage receives the pre-processing phase, where the AGB of *B. planiculmis* using Historical Information Passing Network. The FLOIs employed to enhance the Historical Information Passing Network by predict the neural network's predict the AGB of *B. planiculmis*. Fig 1 depicts the Block diagram proposed methodology.

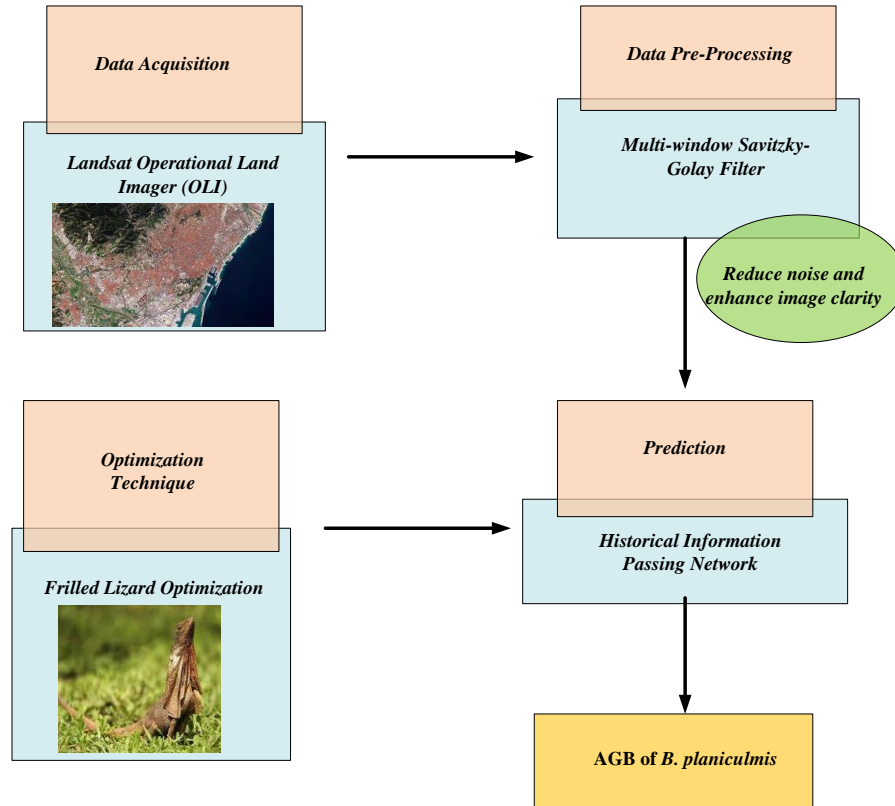


Fig 1: Block diagram of proposed methodology

A. Data Acquisition

In this section input image is taken from the Flickr Material Database [18]. The AGB of *B. planiculmis* was estimated using a Landsat OLI dataset with a 30 m multispectral spatial clarity. The benefits of using Landsat photos include low distribution costs and the ability to get seasonal imagery repeatedly over a brief time span. Two days following the field sample, Landsat traveled over the study region, and the period of data capture coincided with low tide (MSL: 68 cm). Using a criterion matching tool, the standard terrain correction picture (Level 1T) was acquired from the Earth Explorer website. Through the conversion of image digital numbers (DN) into reflectance, the Landsat picture underwent radio metric correction. Dark object removal was used to adjust for atmospheric effects. Erdas Imagine and ENVI were utilized for all image processing.

B. Image Preprocessing Using Multi-Window Savitzky-Golay Filtering

In this section, the input image is pre-processed utilizing MWSGF [19]. It is used to reduce noise and enhance image clarity. Originally developed by Savitzky and Golay, the SG filter is well-known for its ability to smooth data and has found extensive application in a variety of sectors, including analytical chemistry, medicine, and geosciences. The data can be smoothed with an SG filter without losing the majority of its original qualities. Multi-window SG filtering can help remove noise and artifacts, thereby improving the correctness of the mechanism learning models used aimed at analysis. This filtering method is chosen because it provides a balance between noise reduction and preservation of important information in the reflectance data.

The SG sieve is a convolution that simplifies least-squares appropriate and is used to smooth and calculate the derivatives of a series of successive values. Convolution may be considered a moving average filter that is weighted, with weights determined by a polynomial with a degree. The Landsat photos are accessible for repeating seasonal photographs over a brief period of time and may be distributed at a reasonable cost.

$$P(i) = \sum_{k=0}^n a_k i^k \tag{1}$$

Where k signifies the k th heaviness constant of the exponential $P(i)$. In both windows, the next remaining purpose is reduced. By transforming image DN into reflectance, the Landsat picture underwent radiometric correction. In equation (2), the noise was reduced from the image.

$$\delta_n = \sum_{i=-M}^M (P(i) - x[i])^2 = \sum_{i=-M}^M \left(\sum_{k=0}^n a_k i^k - x[i] \right)^2 \tag{2}$$

The polynomial's value $P(i)$ at the vital point ($i = 0$) is the sieve output. In order to calculate the filter output, the window slides point by point. Convolution of the input picture opinions in windows with a secure impulse reply is the analogous technique to this one. Hence, the sieve output can be articulated as shadows, in equation (3), the image clarity was improved.

$$y(k) = \sum_{i=-M}^M \omega_i x[k-i] = \sum_{i=-M}^M \omega_{k-i} x[i] \tag{3}$$

Where $\{\omega_i\}$ means the SG filter's unchanging impulse response. This shows that SG is represented by the weighted regular of the input image points inside a certain frame. filter output in that window. Finally, the MWSGF has enhanced the clarity of the image. Then the Pre-processed image is given to the historical information passing network for prediction.

C. Prediction using Historical Information Passing Network (HIPN)

In this section, a Historical Information Passing Network (HIPN) [20] is discussed. It is used to predict AGB of *B. planiculmis*. HIPN can enhance the performance of tasks such as time-series forecasting, sequential data analysis, or event prediction. The model can learn from past experiences to make more informed decisions or predictions, leading to better overall performance metrics. HIPN enables us to capture sequential patterns and trends, leading to more accurate predictions. This algorithm is particularly well-suited for scenarios where temporal context plays a crucial role, such as time-series forecasting, sequential data analysis, and event prediction. Furthermore, the inclusion of historical data aids in filtering out noise and irrelevant information, improving the network's robustness to noisy data. This not only leads to more reliable predictions but also reduces over fitting tendencies by regularizing the learning process.

In this unit, the aim is to study an unraveled implanting $x_{s,t}$ for object S . Firstly, project $x_{s,t-1}$ onto K seats as follows:

$$h_{s,k} = U_k^T x_{s,t-1} \tag{4}$$

Where $U_k \in R^{d_{in} \times K}$ is the boundary of station k and K is the hyper parameter, It can get the bulge embedding's of K dissimilar mechanisms, i.e. $h_s = \{h_{s,1}, h_{s,2}, \dots, h_{s,k}, \dots, h_{s,k}\}$

The amount of stems and crushed coverage (%) were noted, and plant samples from the quadrat were gathered in order to assess the AGB. As opposed to unlike other graph neural networks, which just include nodes into the graph, Comp GCN uses relation embedding's rather than matrices. So for each multiply $(s, r, o, t-1) \in G(t-1)$, additionally, they must project the entity-relation composition operation's outcomes onto the spaces in the manner described below:

$$c_{o,k} = V_k^T \phi(x_{r,t-1}, x_{o,t-1}) \tag{5}$$

Where $V_k \in R^{d_{in} \times K}$ is the limit of station k , and $\phi(x_r, x_o)$ is the conformation operation, like subtraction, multiplication and circular-correlation, Then it can set K consideration values, and the k -th attention value α_k designates how related the message $\phi(x_r, x_o)$ is to the k -component $h_{s,k}$. The care weight α_k is calculated as follows: Equation (6) predicts the AGB of *B. planiculmis*.

$$\alpha_k = \frac{\exp(\text{Re } LU(W[c_{o,k}; h_{s,k}]))}{\sum_{k'=1}^K \exp(\text{Re } LU(W[c_{o,k'}; h_{s,k'}]))} \tag{6}$$

The AGB of *B. planiculmis* was estimated using Landsat spectral reflectance data and ground observations of plot biomass. Typically, radiation amounts are measured using satellite sensors because of their higher spatial resolution compared to field point sampling coverage. Where $W \in R^{1 \times \frac{2d_{in}}{K}}$ is a transformation matrix that may be used for training, the structural aggregator's update equation is provided as:

$$x_{s,k}^l = \sum_{(r,o') \in N(s)} \alpha_k W_{\lambda(r)}^{l,k} c_{o',k}^{l-1} \tag{7}$$

Here, $W_{\lambda(r)}^{l,k} \in R^{\frac{out}{K} \times \frac{in}{K}}$ is a relation-type limitation about the k -th constituent for the unique, converse also self-loop relations. It tile the K output embedding's $x_{s,k}^L$ to get the physical picture $x_{s,t}$ of entity s at time t , where L is the last layer. And the Comp GCN can consider the embedding's of relatives in the combining procedure, they can also get the refined implanting $x_{r,t}$ for relative r . Finally, HIPN predicted the AGB of *B. planiculmis*. In this work, FLO is employed to optimize the HIPN optimum parameters α_k , and V_k^T . Here FLO is employed for change the weight and bias limit of HIPN.

D. Optimization using Frilled Lizard Optimization (FLO)

In this section, FLO [21] is described. The FLO improved the HIPN weight parameters α_k , and V_k^T in order to improve the suggested RSPB-HIPN-FLO techniques. FLO is designed to explore the search space efficiently, helping to find diverse solutions in complex optimization problems. FLO proves particularly valuable when dealing with complex optimization challenges, offering an alternative avenue where traditional algorithms struggle. Its ability to explore the search space effectively often leads to the discovery of diverse and competitive solutions, potentially converging towards global optima. The idea and inspiration for the creation of FLO are described in this section. Subsequently, the related operation stages are represented mathematically so as to be used to optimization issues.

Step1: Initialization

Set the input parameters to their initial values. In this case, the input parameters are the HIPN weight parameters, which are indicated as α_k, V_k^T

Step2: Random generation

The initialized populations are randomly created by using random generation, which is described by,

$$X = \begin{bmatrix} X_1 \\ \vdots \\ X_i \\ \vdots \\ X_N \end{bmatrix}_{N \times m} = \begin{bmatrix} x_{1,1} & \cdots & x_{1,d} & \cdots & x_{1,m} \\ \vdots & \ddots & \vdots & \ddots & \vdots \\ x_{i,1} & \cdots & x_{i,d} & \cdots & x_{i,m} \\ \vdots & \ddots & \vdots & \ddots & \vdots \\ x_{N,1} & \cdots & x_{N,d} & \cdots & x_{N,m} \end{bmatrix}_{N \times m} \tag{8}$$

Here, X is the FLO population matrix, X_i represents the i^{th} frilled lizard, $x_{i,d}$ denotes its d^{th} measurement in the hunt space, m is an amount of decision variables, N gives the number of frilled lizards.

Step 3: Fitness Function

The outcome is derived from the random response and initialized evaluations. Weight parameter optimization's effects α_k are used in suitability function valuation. It is intended using equation (9)

$$fitness\ function = Optimizing [\alpha_k, V_k^T] \tag{9}$$

Where, α_k denotes the increasing the accuracy, V_k^T represent decreasing the error.

Step 4: Hunting Strategy for Optimizing α_k

One of the most characteristic natural performances of the frilled lizard is a hunting approach of this animal. The frilled lizard is a sit-and-wait predator that attacks its prey after seeing it. The simulation of frilled lizard's movement near the prey leads to extensive changes in the population's location inside the problem-solving

domain, which in turn boosts the global search procedure's exploratory potential. Based on the frilled lizard's hunting technique, the population individuals' location in the problem's solution space is efficient during the first phase of FLO.

$$CP_i = \{\alpha_k : F_k < F_i \text{ and } k \neq i\}, \quad i = 1, 2, \dots, N \text{ and } k \in \{1, 2, \dots, N\} \quad (10)$$

Here, CP is the candidate preys set for the i^{th} frilled lizard, α_k is the populace affiliate with a healthier impartial purpose worth than the i^{th} frilled lizard, and F_k is its impartial purpose value.

$$X_i = \begin{cases} X_i^{p1}, & F_i^{p1} < F_i \\ X_i, & \text{else} \end{cases} \quad (11)$$

Here, X_i^{p1} is the new recommended location of the i^{th} frilled lizard founded on first phase of FLO, F_i^{p1} is its impartial function worth.

Step 5: Moving up the Tree for Optimizing V_k^T

After feeding, the frilled lizard retreats to the top of a tree near its position. Simulating the movement of the frilled lizard to the top of the tree increases the misuse capability of the local search procedure by causing slight changes in the Population individuals' positions in the problem's solution space. In the second phase of FLO, the population members' locations inside the solution space are updated. It depending on the frilled lizard's retreat strategy to the top of the tree following feeding.

$$x_{i,d}^{p2} = x_{i,d} + (1-2r) \cdot \frac{(ub_d - lb_d)}{V_k^T}, \quad i = 1, 2, \dots, N, \quad d = 1, 2, \dots, m, \quad \text{and } t = 1, 2, \dots, T \quad (12)$$

$$X_i = \begin{cases} X_i^{p2}, & F_i^{p2} < F_i \\ X_i, & \text{else} \end{cases} \quad (13)$$

Here, X_i^{p2} denotes the new proposed location of the i^{th} frilled lizard founded on the second stage of FLO, F_i^{p2} is its impartial function value. T describes a maximum number of iterations of the process.

Step 6: Update the Best Solution

If the ideal outcome is got then the procedure is end.

Step 7: Termination

If the key is the best, the procedure terminates; if not, it loops back to the step 3 suitability computations, processing each level after that until a solution is discovered.

III. RESULT AND DISCUSSION

In this manuscript, outcomes of proposed method are discussed in this section. Next, Python is used to simulate the suggested method under the specified performance metrics. The suggested RSPB-HIPN-FLO approach's result is examined using current systems such as PSHRS-ANN, RSICS-DNN and SYMRS-GOA respectively.

A. Performance Metrics

A comparative analysis of the performance metrics, including accuracy, precision additionally included are the Correlation Coefficient, Mean Absolute Error, and Root Mean Squared Error.

1) Accuracy

It is the ratio of the amount of properly predicted entries to the entire amount of predictions for a given dataset. It is quantified using an equation. (14),

$$Accuracy = \frac{(TP + TN)}{(TP + FP + TN + FN)} \quad (14)$$

Where, TP is signifies true positive, TN s signifies as true negative, FP is represents false positive, and FN is represents untrue adverse.

2) Precision

A statistic called precision counts how many positive predictions were made correctly. This is calculated using equation (15),

$$Precision = \frac{TP}{(TP + FP)} \tag{15}$$

3) Correlation Coefficient

The correlation constant (r) extracted from every model and used in the forecasts of live biomass.

$$r = \frac{\sum_{i=1}^N (p_i - \overline{p_i})(p_{situ} - \overline{p_{situ}})}{\sqrt{\sum_{i=1}^N (p_i - \overline{p_i})^2} \sqrt{\sum_{i=1}^N (p_{situ} - \overline{p_{situ}})^2}} \tag{16}$$

Where p_i a model is forecast; p_{situ} is the in-situ biomass dimension; $\overline{p_i}$ and $\overline{p_{situ}}$ are the average of the in-situ biomass measurements and the model forecasts.

4) Mean Absolute Error

The mean total error indicates the average amount of error among the expected and real numbers. It is computed by captivating the average of the total differences among the expected and observed standards.

$$MAE = \frac{1}{N} \sum_{i=1}^N |p_i - p_{situ}| \tag{17}$$

N is the total amount of matched samples

5) Root Mean Squared Error

When the differences are squared before calculating the square root of the regular, the root nasty shaped error measure represents the regular size of the errors among the predictable and actual values. Likened to MAE, it assigns greater weight to bigger mistakes.

$$RMSE = \sqrt{\frac{1}{N} \sum_{i=1}^N (p_i - p_{situ})^2} \tag{18}$$

B. Performance Analysis

Fig 2 to 6 depicts the simulated outcomes of the suggested RSPB-HIPN-FLO technique. The suggested RSPB-HIPN-FLO approach is then contrasted with the current PSHRS-ANN, RSICS-DNN and SYMRS-GOA methods respectively.

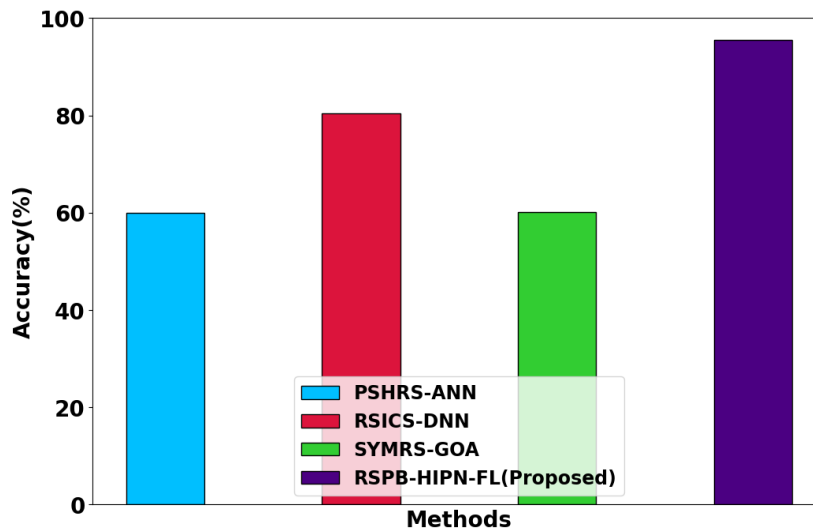


Fig 2: Performance analysis of accuracy

The Presentation analysis of correctness method is depicts in Fig 2. The presentation of the proposed technique results in accuracy that are 23.52%, 21.72%, 24.92%, higher for predicting the AGB of B.

planiculmis, when evaluated to the existing PSHRS-ANN, RSICS-DNN and SYMRS-GOA models respectively.

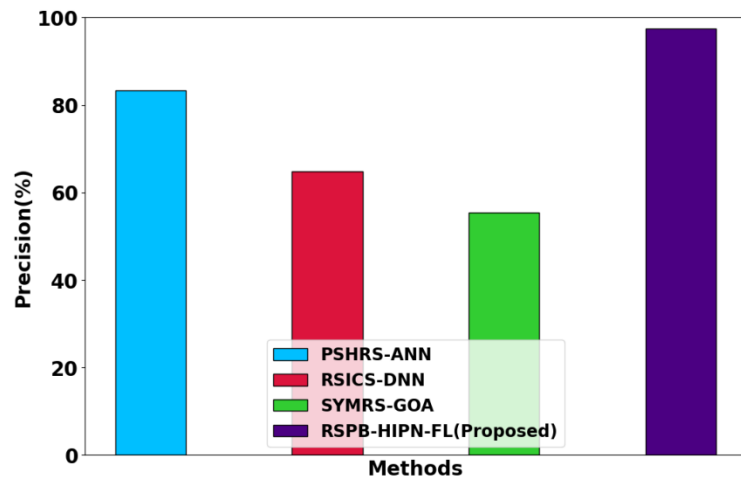


Fig 3: Performance analysis of precision

The Presentation examination of exactness method is depicts in Fig 3. The presentation of the proposed technique results in precision that are 23.52%, 22.72%, 21.92%, higher for predicting the AGB of *B. planiculmis*, when evaluated to existing PSHRS-ANN, RSICS-DNN and SYMRS-GOA models respectively.

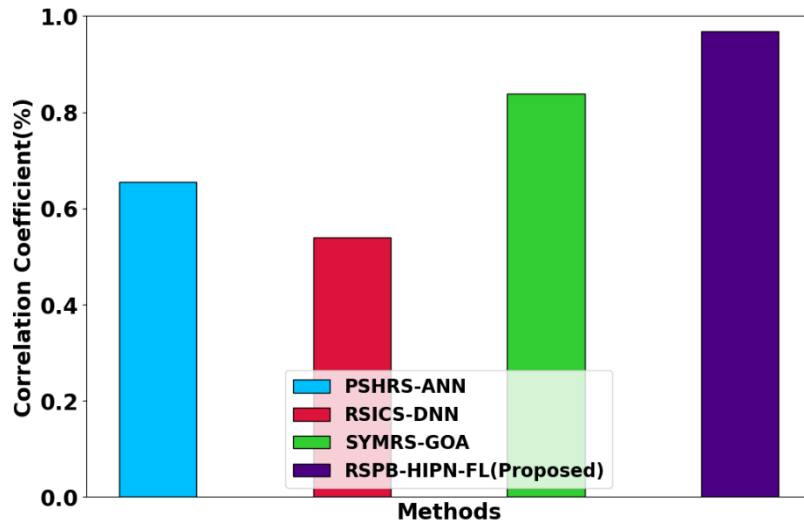


Fig 4: Performance analysis of Correlation Coefficient

The Performance analysis of Association Coefficient method is depicts in Fig 4. The presentation of the suggested technique results in precision that are 21.58%, 24.70%, 23.92%, higher for predicting the AGB of *B. planiculmis*, when evaluated to existing PSHRS-ANN, RSICS-DNN and SYMRS-GOA models respectively.

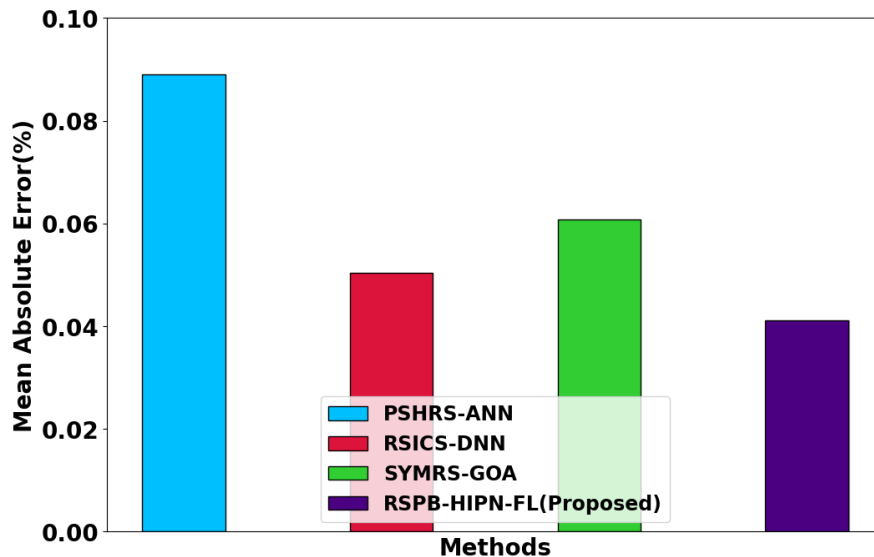


Fig 5: Performance analysis of Mean Absolute Error

The Presentation examination of Mean Complete Mistake method is depicts in Fig 5. The presentation of the suggested technique results in precision that are 20.57%, 21.72%, 22.93%, higher for predicting the AGB of *B. planiculmis*, when evaluated to the existing PSHRS-ANN, RSICS-DNN and SYMRS-GOA models respectively.

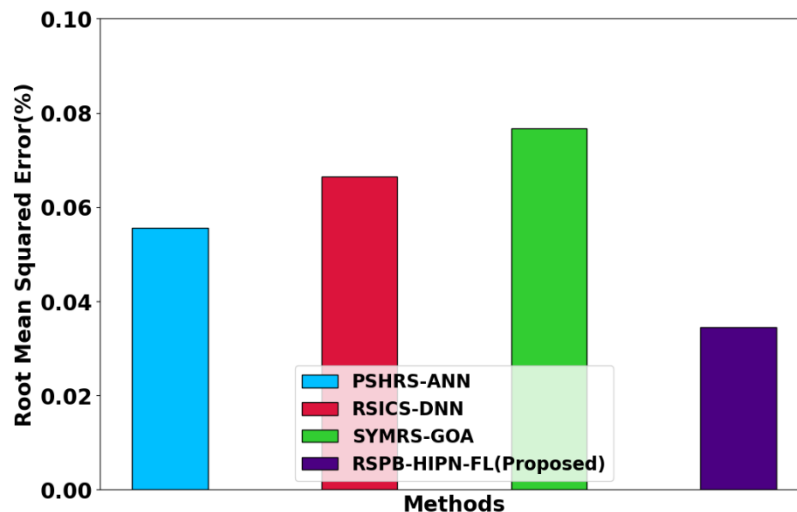


Fig 6: Performance analysis of Mean Absolute Error

The Performance examination of Mean Absolute Error method depicts in Fig 6. The presentation of the future technique consequences in precision that are 24.58%, 21.71%, 22.90%, higher for predicting the AGB of *B. planiculmis*, when evaluated to the existing PSHRS-ANN, RSICS-DNN and SYMRS-GOA models respectively.

C. Discussion

The comprehensive performance analysis demonstrates the significant advancements achieved by the proposed methodology in accurately predicting the (*B. planiculmis*), a vital species for wetland restoration efforts in the MNRR, Northeast China. Through the integration of multivariate regression techniques with innovative algorithms like Historical Information Passing Networks (HIPNs) optimized by FLO, the model showcases remarkable improvements in accuracy, precision, and error metrics compared to existing approaches such as PSHRS-ANN, RSICS-DNN, and SYMRS-GOA. Leveraging preprocessing techniques like Multi-window Savitzky-Golay Filtering (MWSGF) enhances data clarity, while the adoption of FLO ensures adaptive optimization strategies for parameter tuning, thereby elevating prediction accuracy. The proposed RSPB-HIPN-FLO framework offers a promising avenue for effective biomass estimation, highlighting its potential for informed decision-making in wetland management and conservation initiatives.

IV. CONCLUSION

In this section, Prediction modeling of AGB of *B. planiculmis* remote sensing monitoring (RSPB-HIPN-FLO) was successfully implemented. The proposed RSPB-HIPN-FLO method is executed in the Python working platform utilizing the dataset of OLI dataset. The performance of the RSPB-HIPN-FLO method contains accuracy, precision, Association Coefficient, Root Mean Squared Error and Mean Total Error. The planned RSPB-HIPN-FLO technique attains 23.52%, 21.72% and 24.92% higher accuracy predictions AGB of *B. planiculmis* respectively. The proposed RSPB-HIPN-FLO method attains 23.52%, 22.72% and 21.92% higher precision for predictions AGB of *B. planiculmis* respectively. The proposed RSPB-HIPN-FLO method attains 24.58%, 21.71% and 22.90% higher Association Coefficient for predictions AGB of *B. planiculmis* respectively. The future work could involve refining the machine learning models used for remote sensing monitoring and prediction of AGB of *B. planiculmis*. This could include exploring advanced algorithms, integrating additional data sources, improving model accuracy and efficiency, and expanding the scope of applications for the predictive models. Additionally, there could be a focus on field validation of the models to ensure their reliability in real-world scenarios.

Acknowledgement :

National Key R&D Program: Research on the Mechanism of Malignant Weed Catastrophe and Sustainable Prevention and Control Technologies, Number: 2023YFD1400502.

REFERENCE:

- [1] Ning, Y., Li, Y., Lin, H. Y., Kang, E. Z., Zhao, Y. X., Dong, S. B., ... & Li, C. Y. (2024). Chromosome-scale genome assembly for clubrush (*Bolboschoenus planiculmis*) indicates a karyotype with high chromosome number and heterogeneous centromere distribution. *Genome Biology and Evolution*, *16*(3), evae039.
- [2] Ying, L., Maohua, M., Zhi, D., Bo, L., Ming, J., Xianguo, L., & Yanjing, L. (2023). Light-acquisition traits link aboveground biomass and environment in inner saline-alkaline herbaceous marshes. *Science of the Total Environment*, *857*, 159660.
- [3] Hung, S. H. W., Yeh, P. H., Huang, T. C., Huang, S. Y., Wu, I. C., Liu, C. H., ... & Huang, C. C. (2024). A cyclic dipeptide for salinity stress alleviation and the trophic flexibility of endophyte provide insights into saltmarsh plant-microbe interactions. *ISME Communications*, *4*(1), ycae041.
- [4] Khalifa, A., & Alsowayeh, N. (2023). Whole-Genome Sequence Insight into the Plant-Growth-Promoting Bacterium *Priestiafilamentosa* Strain AZC66 Obtained from *Zygothylum coccineum* Rhizosphere. *Plants*, *12*(10), 1944.
- [5] Ning, Y., Li, Y., Dong, S. B., Yang, H. G., Li, C. Y., Xiong, B., ... & Xia, X. F. (2023). The chromosome-scale genome of *Kobresia myosuroides* sheds light on karyotype evolution and recent diversification of a dominant herb group on the Qinghai-Tibet Plateau. *DNA Research*, *30*(1), dsac049.
- [6] Arce, W. A., & Achá, D. (2023). Allometric determinations in the early development of *Schoenoplectus californicus* to monitor nutrient uptake in constructed wetlands. *Ecohydrology & Hydrobiology*.
- [7] Wu, H., Dong, S., Wang, Y., Wang, L., & Rao, B. (2023). Niche Characteristics of *Alternanthera philoxeroides*-Invaded Plant Communities in Heterogeneous Habitats and Their Latitudinal Trends. *Diversity*, *15*(5), 651.
- [8] Ying, L., Yanfeng, W., Wenzhou, W., Zhi, D., Maohua, M., Ping, H., ... & Yanjing, L. (2023). Plant-plant interactions vary greatly along a flooding gradient in a dam-induced riparian habitat. *Frontiers in Plant Science*, *14*, 1290776.
- [9] Ding, S., Zou, Y., & Yu, X. (2023). Freeze-thaw cycles alter the growth sprouting strategy of wetland plants by promoting denitrification. *Communications Earth & Environment*, *4*(1), 57.
- [10] Yu, Z. C., Zheng, X. T., He, W., Lin, W., Yan, G. Z., Zhu, H., & Peng, C. L. (2023). Different responses of macro- and microelement contents of 41 subtropical plants to environmental changes in the wet and dry seasons. *Journal of Plant Ecology*, *16*(6), rtad027.
- [11] Papp, L., Van Leeuwen, B., Szilassi, P., Tobak, Z., Szatmári, J., Árvai, M., ... & Pásztor, L. (2021). Monitoring invasive plant species using hyperspectral remote sensing data. *Land*, *10*(1), 29.
- [12] Ko, J., Shin, T., Kang, J., Baek, J., & Sang, W. G. (2024). Combining machine learning and remote sensing-integrated crop modeling for rice and soybean crop simulation. *Frontiers in Plant Science*, *15*, 1320969.
- [13] Lu, J., Fu, H., Tang, X., Liu, Z., Huang, J., Zou, W., ... & Li, J. (2024). GOA-optimized deep learning for soybean yield estimation using multi-source remote sensing data. *Scientific Reports*, *14*(1), 7097.
- [14] Javaid, M., Haleem, A., Khan, I. H., & Suman, R. (2023). Understanding the potential applications of Artificial Intelligence in Agriculture Sector. *Advanced Agrochem*, *2*(1), 15-30.
- [15] Hwang, H. H., Chien, P. R., Huang, F. C., Yeh, P. H., Hung, S. H. W., Deng, W. L., & Huang, C. C. (2022). A plant endophytic bacterium *Priestia megaterium* Strain BP-R2 Isolated from the Halophyte *Bolboschoenus planiculmis* enhances plant growth under salt and drought stresses. *Microorganisms*, *10*(10), 2047.

- [16] Yang, H., Kim, J. H., & Lee, E. J. (2021). Impacts of tidal restriction caused by embankments on the plastic growth responses of *Bolboschoenusplaniculmis* in Korea. *Regional Studies in Marine Science*, *41*, 101616.
- [17] Yang, H., Kim, J. H., & Lee, E. J. (2020). Effects of tides on interspecific interactions and plastic growth responses of *Bolboschoenusplaniculmis*. *Flora*, *264*, 151568.
- [18] <https://www.usgs.gov/centers/eros/science/usgs-eros-archive-landsat-archives-landsat-8-9-olitirs-collection-2-level-2>
- [19] Liu, W., Wang, H., Xi, Z., & Zhang, R. (2023). Smooth Deep Learning Magnetotelluric Inversion based on Physics-informed Swin Transformer and Multi-Window Savitzky-Golay Filter. *IEEE Transactions on Geoscience and Remote Sensing*.
- [20] He, Y., Zhang, P., Liu, L., Liang, Q., Zhang, W., & Zhang, C. (2024). HIP network: historical information passing network for extrapolation reasoning on temporal knowledge graph. *arXiv preprint arXiv:2402.12074*.
- [21] Falahah, I. A., Al-Baik, O., Alomari, S., Bektemyssova, G., Gochhait, S., Leonova, I., ...&Dehghani, M. (2024). Frilled Lizard Optimization: A Novel Nature-Inspired Metaheuristic Algorithm for Solving Optimization Problems.